Analysis of ArH^+, H_3^+, OH^+, and H_2O^+ Observations to Estimate the Cosmic-Ray Ionization Rate Using Comprehensive Diffuse Cloud Models

1) ArH^+ - history, formation/destruction

2) Models − geometry, physical processes

3) Results and comparisons

Wolfire, M.G & Neufeld, D. A.

Thanks! NASA/ADAP

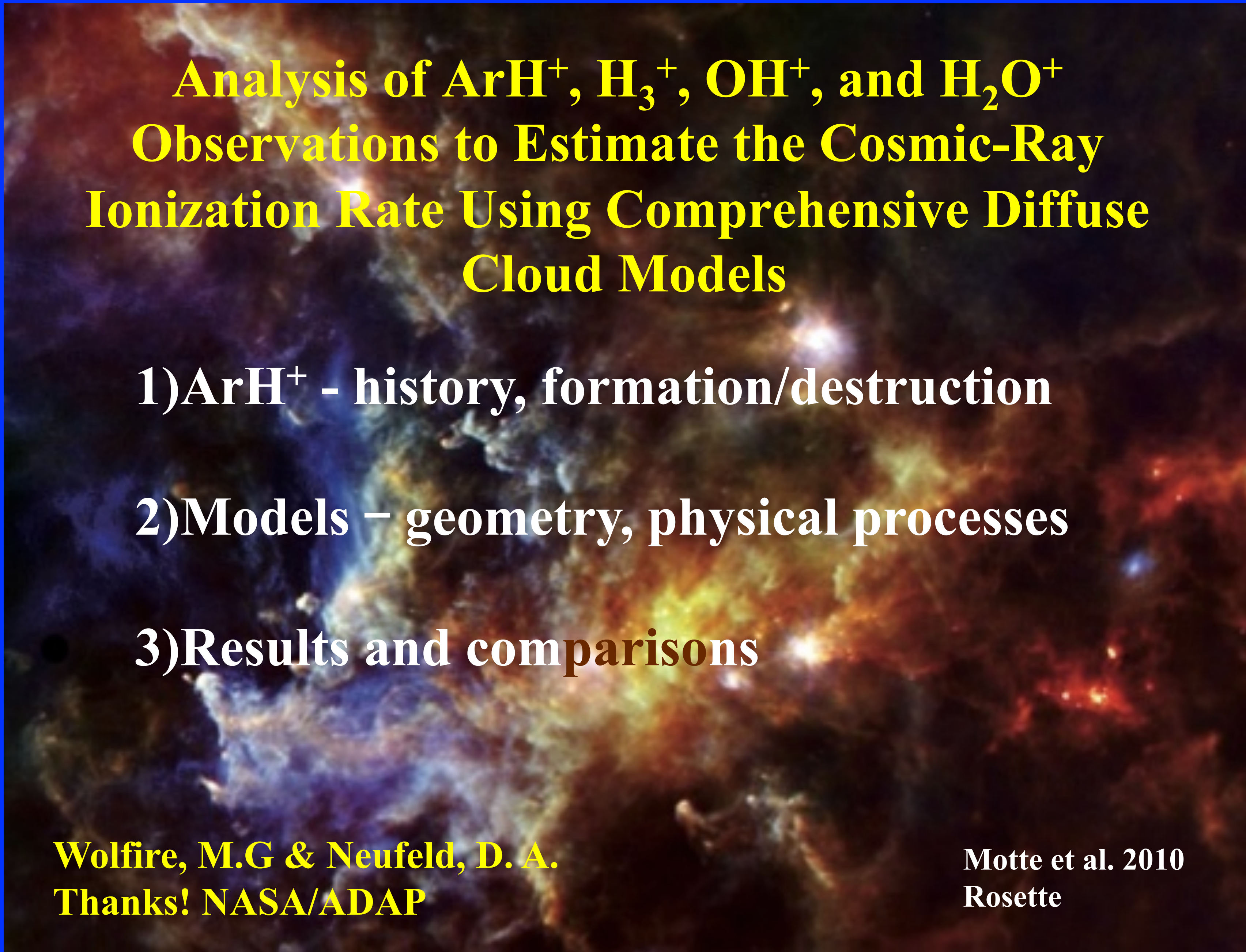

Motte et al. 2010
Rosette

Argonium - ArH^+

Observed by PRISMAS and HEXOS in absorption towards SgrB2 but unidentified – Muller et al. 2013

Observed in emission in Crab Nebula identified as $^{36}ArH^+$ - Barlow et al. 2013

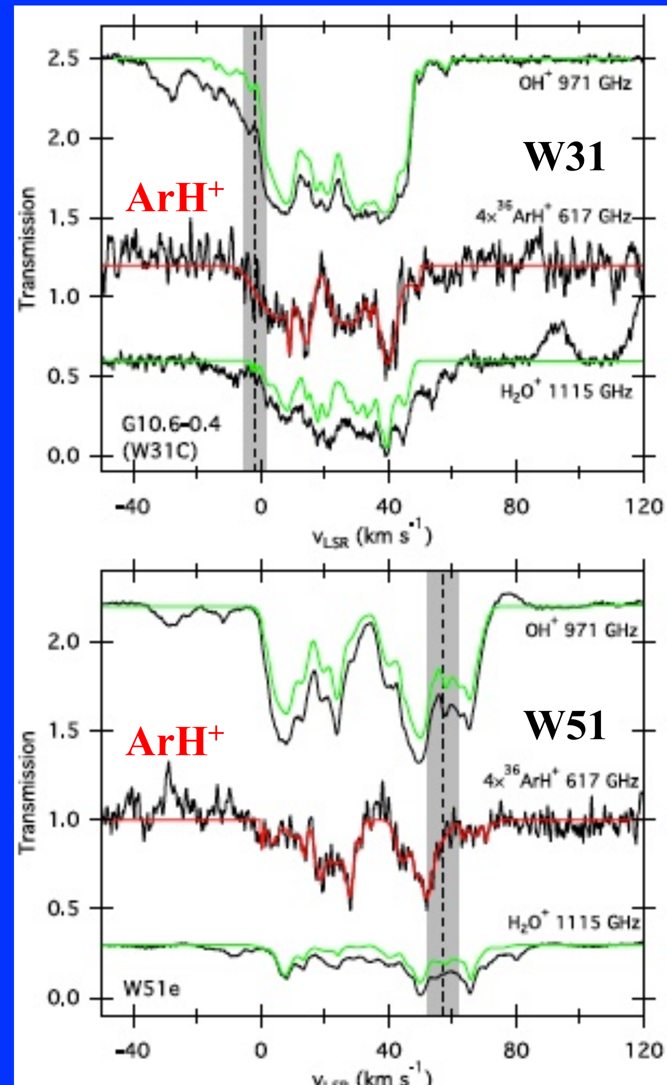

Schilke et al. 2014

See also Poster 22 on ArH^+ from Crab Nebula

Argonium - ArH^+

Observed by PRISMAS and HEXOS in absorption towards SgrB2 but unidentified – Muller et al. 2013

Observed in emission in Crab Nebula identified as $^{36}ArH^+$ - Barlow et al. 2013

Formation:

$$Ar + CR \rightarrow Ar^+ + e$$

$$Ar^+ + H_2 \rightarrow ArH^+ + H$$

Destruction:

$$ArH^+ + O \rightarrow Ar + OH^+$$

$$ArH^+ + H_2 \rightarrow Ar + H_3^+$$

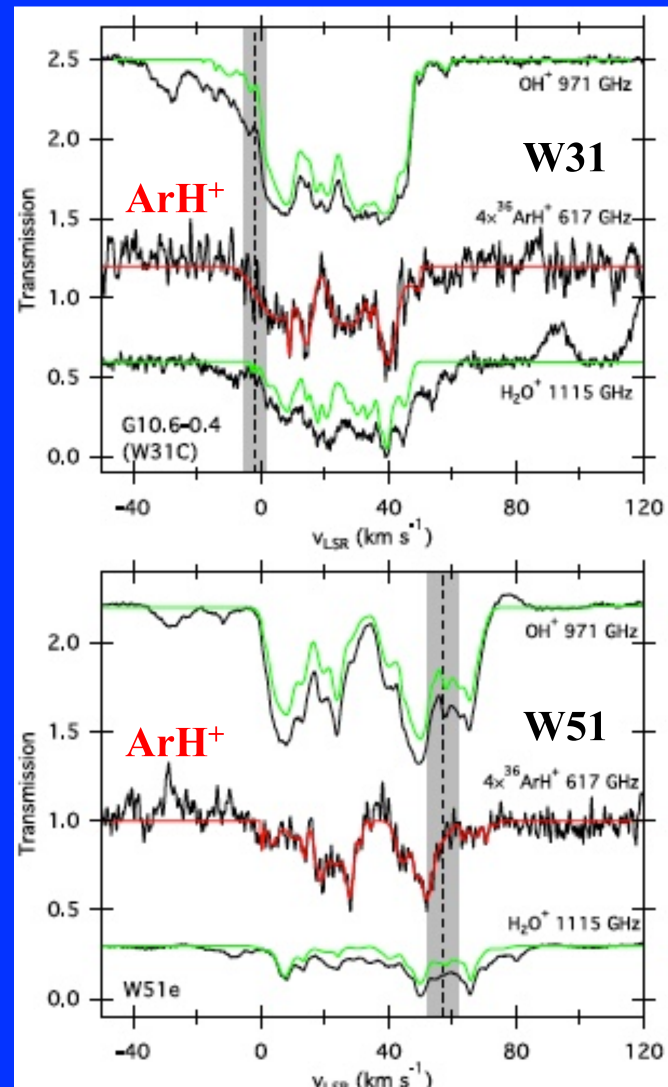

Schilke et al. 2014

See also Poster 22 on ArH^+ from Crab Nebula

Argonium - ArH^+

Observed by PRISMAS and HEXOS in absorption towards SgrB2 but unidentified – Muller et al. 2013

Observed in emission in Crab Nebula identified as $^{36}ArH^+$ - Barlow et al. 2013

Formation:

$$\mathrm{Ar} + CR \rightarrow \mathrm{Ar}^+ + e$$

$$\mathrm{Ar}^+ + \mathrm{H}_2 \rightarrow \mathrm{ArH}^+ + \mathrm{H}$$

Destruction:

$$\mathrm{ArH}^+ + \mathrm{O} \rightarrow \mathrm{Ar} + \mathrm{OH}^+$$

$$\mathrm{ArH}^+ + \mathrm{H}_2 \rightarrow \mathrm{Ar} + \mathrm{H}_3^+$$

See also Poster 22 on ArH^+ from Crab Nebula

2- Sided PDR model

$A_V(tot) = 0.3$

Abundance per H nuclei

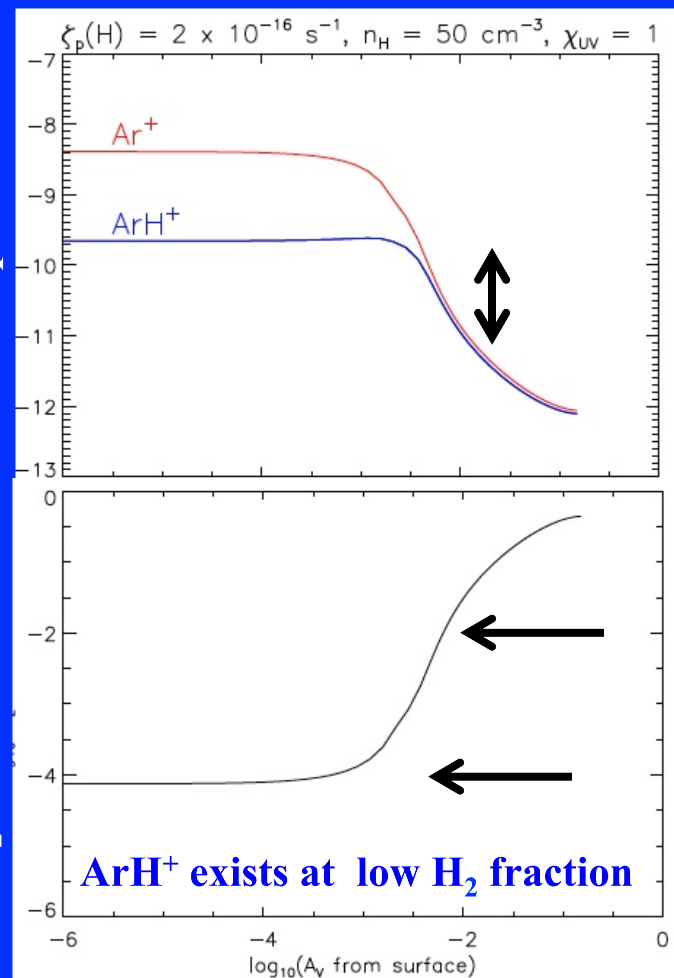

H_2 fraction

log A_V

Schilke et al. 2014

Two-Sided PDR Models

$\chi / 2,\ \zeta$ →

n = constant

T = thermal balance

n_i = steady state

ArH^+, OH^+, H_2O^+, H_3^+, e, H^+, H_2

← **Av(tot)** →

← $\chi / 2,\ \zeta$

1)T varies with inputs and Av

2)e varies with inputs and Av

3)H, H_2 varies with inputs and Av

Parameter Grid

$\chi / n_{50} = 0.05$ to 10 $\quad n = n_{50}\, 50\ \mathrm{cm}^{-3}$

$\zeta_p(\mathrm{H}) / n_{50} = 6\mathrm{x}10^{-3}$ to 60 (x $10^{-16} s^{-1}$)

$A_{\mathrm{v}}(\mathrm{tot}) = 3\mathrm{x}10^{-4}$ to 8 mag

$Z = 1,\ 2$

$n_{50} = 1$

ArH^+, HCl^+, H_2Cl^+, OH^+, H_2O^+ Neufeld & Wolfire 2016

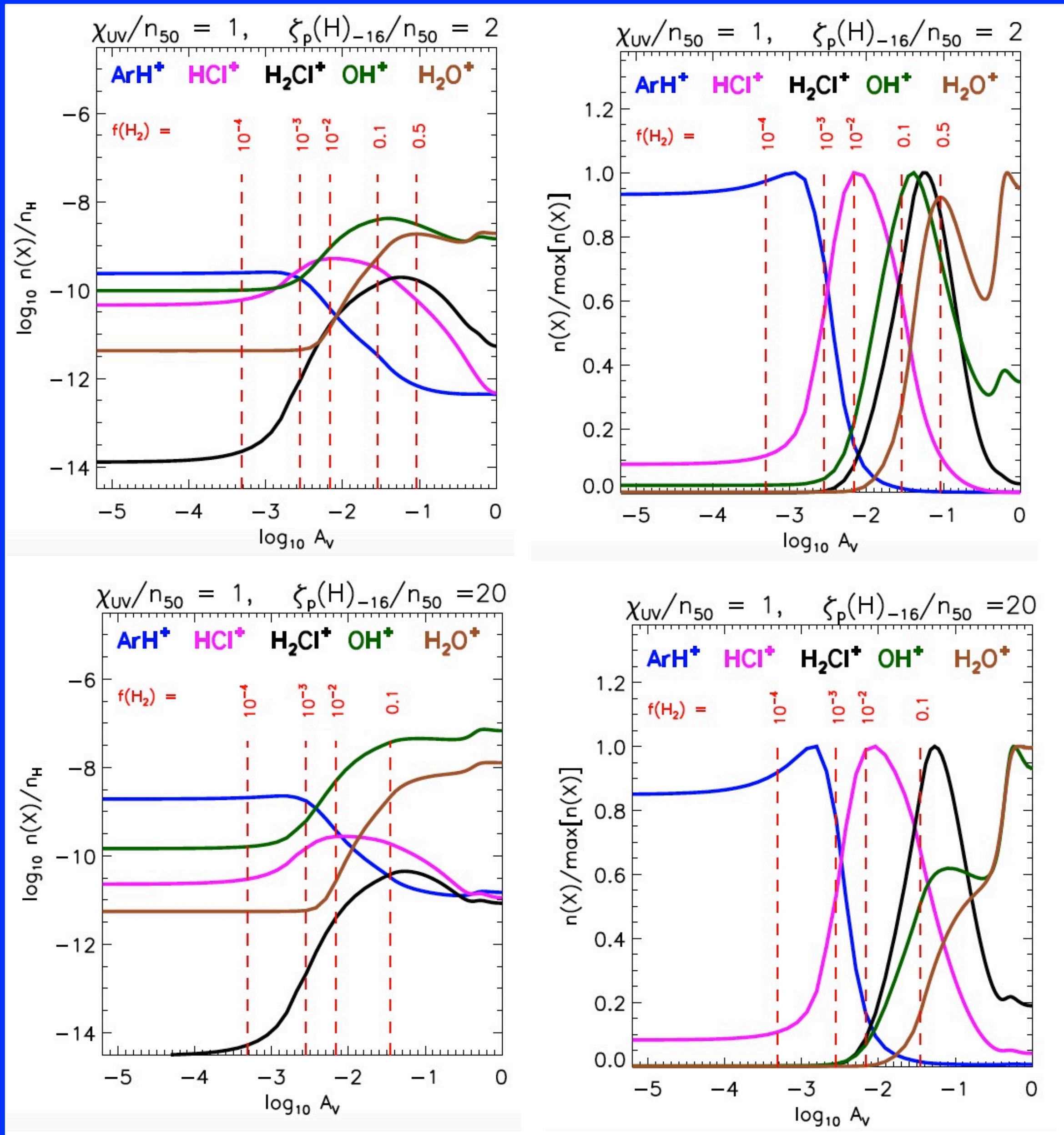

H_2O^+
H_2Cl^+
OH^+
HCl^+
ArH^+

$f(H_2)$ ↑

ArH^+ in small clouds of Av(tot) < 0.02 and $f(H_2) \sim 10^{-5} - 10^{-2}$

OH^+, H_2O^+ in larger clouds and higher $f(H_2)$

Higher CRIR more ArH^+, OH^+, H_2O^+

OH^+, H_2O^+
22 samples

OH^+, H_2O^+, ArH^+
15 samples

H_3^+
7 samples

One component model
All HI in OH^+, H_2O^+
(large) clouds

Indriolo et al. 2015: OH^+, H_2O^+
Winkel et al. 2017: HI

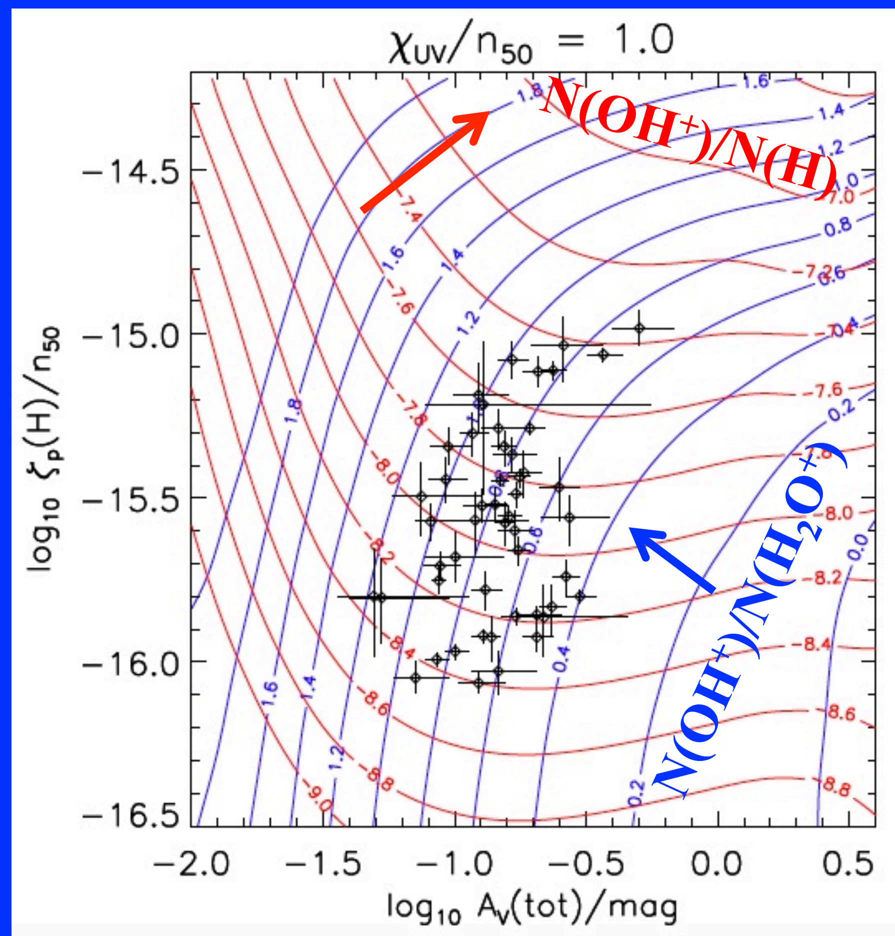

Neufeld & Wolfire 2016, in prep

OH^+, H_2O^+
22 samples

OH^+, H_2O^+, ArH^+
15 samples

H_3^+
7 samples

Two component model
Large OH^+, H_2O^+ cloud
and small ArH^+ cloud

Both have the same
cosmic-ray ionization rates

Up to 50% HI in ArH^+
clouds with remaining
HI in OH^+, H_2O^+ clouds.

$$\Delta[\log_{10} \zeta_p(\mathrm{H}) / n_{50}] = 0.15 \ \ \mathrm{dex}$$

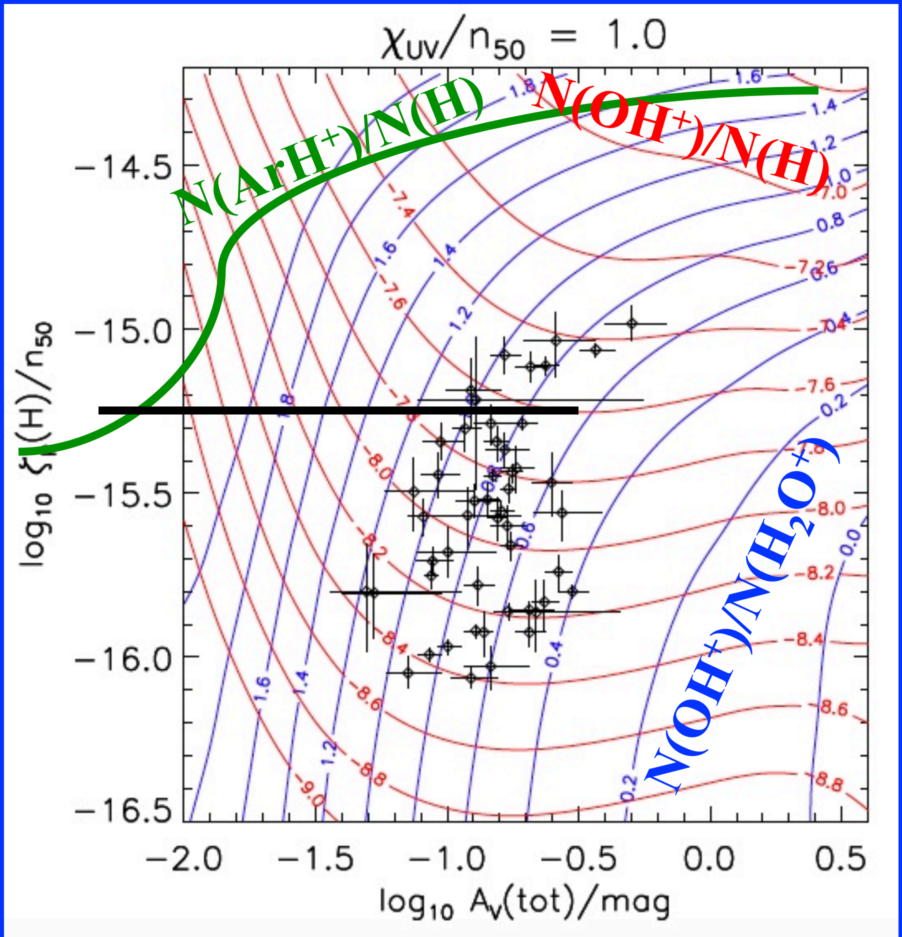

Neufeld & Wolfire 2016, in prep

H_3^+ Clouds

Indriolo & McCall 2012: 23 H_3^+ clouds

6 UV $N(H_2)$ observations

17 $N(H_2)$ from CH, E(B-V)

Albertsson et al. 2014: 3 H_3^+ clouds

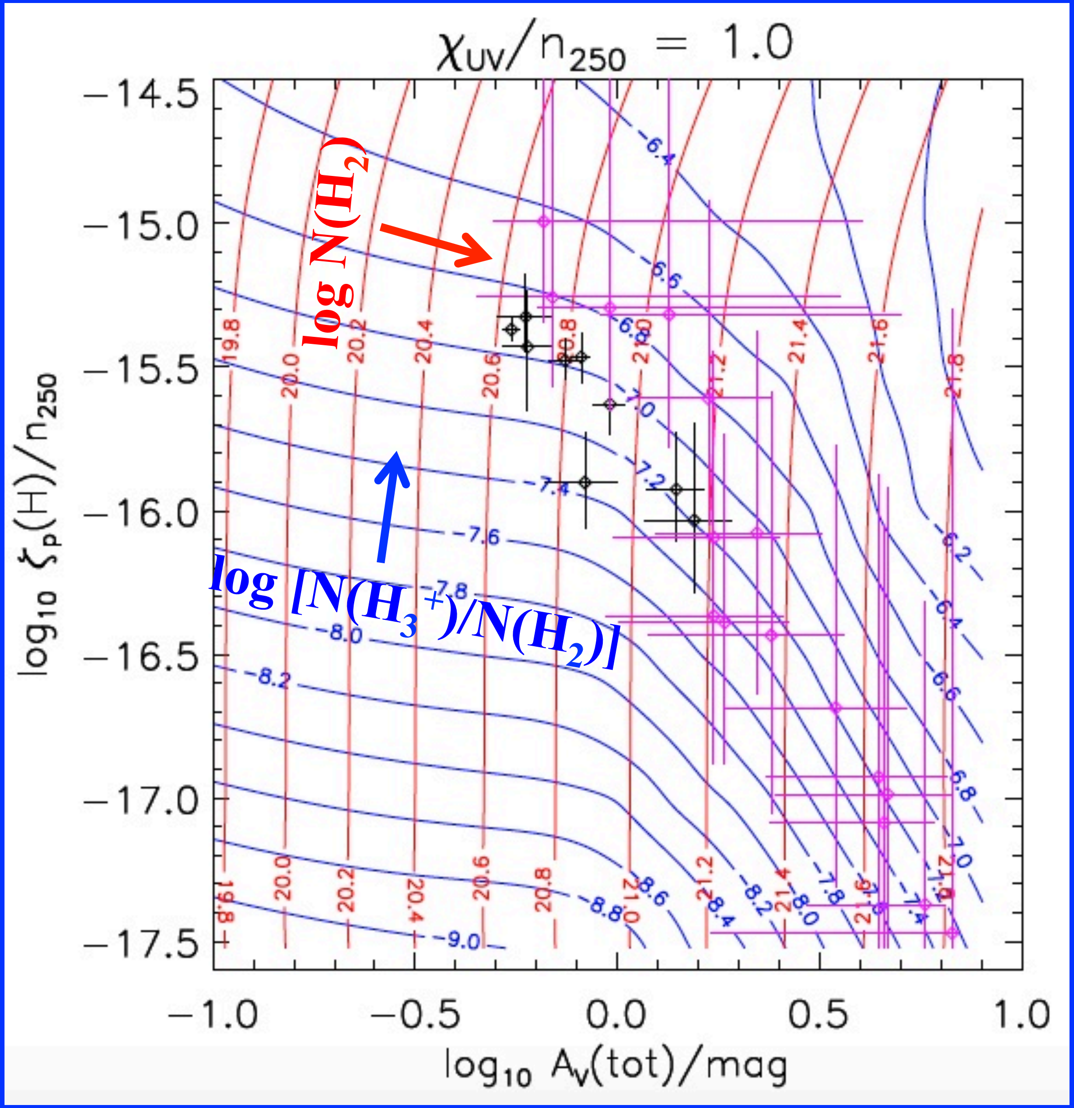

Neufeld & Wolfire 2016, in prep

7 samples H_3^+ with $N(H_2)$ and n from observations

$<\log_{10}[\zeta_p(\mathrm{H})]>$	(Present Work)	-15.63 ± 0.09
$10^{<\log_{10}[\zeta_p(\mathrm{H})]>}/10^{-16}\ \mathrm{s}^{-1}$	(Present Work)	2.3 ± 0.6
$10^{<\log_{10}[\zeta_p(\mathrm{H})]>}/10^{-16}\ \mathrm{s}^{-1}$	(IM12)	1.9
$\sigma_{\mathrm{Best\ Estimate}}[\log_{10}[\zeta_p(\mathrm{H})]]$	(Present Work)	0.23
$\sigma_{\mathrm{True}}[\log_{10}[\zeta_p(\mathrm{H})]]$	(Present Work)	0.09

37 samples OH^+, H_2O^+ with ArH^+ and $\chi/n_{50} = 1$

$<\log_{10}[\zeta_p(\mathrm{H})/n_{50}]>$	(Present Work)	-15.34 ± 0.05
$10^{<\log_{10}[\zeta_p(\mathrm{H})]/n_{50}>}/10^{-16}\ \mathrm{s}^{-1}$	(Present Work)	4.6 ± 0.5
$10^{<\log_{10}[\zeta_p(\mathrm{H})]/n_{50}>}/10^{-16}\ \mathrm{s}^{-1}$	(I15)	1.8
$\sigma_{\mathrm{Best\ Estimate}}[\log_{10}[\zeta_p(\mathrm{H})/n_{50}]]$	(Present Work)	0.29
$\sigma_{\mathrm{True}}[\log_{10}[\zeta_p(\mathrm{H})/n_{50}]]$	(Present Work)	0.23

7 samples H_3^+ with $N(H_2)$ and n from observations

$< \log_{10}[\zeta_p(\mathrm{H})] >$	(Present Work)	-15.63 ± 0.09
$10^{<\log_{10}[\zeta_p(\mathrm{H})]>} / 10^{-16}\ \mathrm{s}^{-1}$	(Present Work)	2.3 ± 0.6
$10^{<\log_{10}[\zeta_p(\mathrm{H})]>} / 10^{-16}\ \mathrm{s}^{-1}$	(IM12)	1.9
$\sigma_{\mathrm{Best\ Estimate}}[\log_{10}[\zeta_p(\mathrm{H})]]$	(Present Work)	0.23
$\sigma_{\mathrm{True}}[\log_{10}[\zeta_p(\mathrm{H})]]$	(Present Work)	0.09

37 samples OH^+, H_2O^+ with ArH^+ and $\chi/n_{50} = 50/33$, n = 33

$< \log_{10}[\zeta_p(\mathrm{H}) / n_{50}] >$	(Present Work)	-15.34 ± 0.05
$10^{<\log_{10}[\zeta_p(\mathrm{H})]>} / 10^{-16}\ \mathrm{s}^{-1}$	(Present Work)	2.2 ± 0.3
$10^{<\log_{10}[\zeta_p(\mathrm{H})]/n_{50}>} / 10^{-16}\ \mathrm{s}^{-1}$	(I15)	1.8
$\sigma_{\mathrm{Best\ Estimate}}[\log_{10}[\zeta_p(\mathrm{H}) / n_{50}]]$	(Present Work)	0.29
$\sigma_{\mathrm{True}}[\log_{10}[\zeta_p(\mathrm{H}) / n_{50}]]$	(Present Work)	0.23

Conclusions

We analyzed OH^+, H_2O^+, ArH^+ and HI observations using our 2-sided PDR model to find CRIR/n_{50} = $4.6\pm0.5\times10^{-16}$ s^{-1} (with $\chi/n_{50} = 1$).

With n = 33, CRIR = $2.2\pm0.3\times10^{-16}$ s^{-1}

We analyzed H_3^+ and H_2 observations using our 2-sided PDR model to find CRIR = $2.3\pm0.6\times10^{-16}$ s^{-1}

Both have quite small cloud-to-cloud variations

Diffuse atomic and diffuse molecular estimates are in agreement